

## Sediment records of past anthropogenic environmental changes in a barrier reef lagoon (Papeete, Tahiti, French Polynesia)

R. Fichez <sup>a,\*</sup>, P.A. Harris <sup>b</sup>, J.M. Fernandez <sup>b,c</sup>, C. Chevillon <sup>b</sup>, C. Badie <sup>d</sup>

<sup>a</sup> Centre d'Océanologie de Marseille, Station Marine d'Endoume, Rue de la Batterie des Lions, 13007 Marseille, France

<sup>b</sup> Centre IRD de Noumea, BP A5 Nouméa, New Caledonia, France

<sup>c</sup> CEN, DESD/SEP/LCCM, BP1 13108 Saint Paul lez Durance, France

<sup>d</sup> L.E.S.E., BP 519 Papeete, Tahiti, French Polynesia, France

One of the main interests in reconstructing the evolution of past environmental conditions is to place the present environmental situation in its historical context. Fine-grained sediments with large adsorption potential represent a good repository for environmental tracers (Valette-Silver, 1993) and during the past decade, geochronology studies combined with the analysis of environmental tracers in sediments have provided valuable information on the respective contribution of marine, terrestrial and anthropogenic inputs through the last century. Rapid modifications in the nature and quantity of deposited sediments are a major source of environmental changes (Chenhall et al., 1995) and sedimentary records have been conclusively used to infer the history of anthropogenic effects such as metal inputs (Zwolsman et al., 1993; Grousset et al., 1999), discharge of organic contaminants (Gerritse et al., 1995; Wakeham, 1996) or nutrient enrichment (Cornwell et al., 1996; Harris et al., 2001).

This paper presents geochronology, sedimentology and geochemical results from two sediment cores sampled in the lagoon surrounding the city and harbour of Papeete, Tahiti, French Polynesia. Beyond local interest, the barrier reef of Papeete is a good example of the environmental problems that Pacific Island States are currently facing. In these countries, populations tend to concentrate in coastal urban areas located on high islands where barrier reefs often delimit small lagoons which are very sensitive to enhanced terrigenous and anthropogenic inputs. Additionally, very few data on past environmental conditions are available in Tahiti as in most Pacific island states (Hutchings et al., 1994; Aubanel et al., 1998). Therefore, information gained from sedimentary records may represent an especially valuable approach to compensate for such a paucity of information. Previous work conducted on the geochemistry of phosphorus in Papeete harbour proved that significant information could be gained on past environmental changes (Harris et al., 2001). Our present work combines results on <sup>210</sup>Pb geochronology, grain size,

carbonate content and metal concentrations in sediments in order to assess the significance of additional terrigenous inputs due to land erosion and direct release of anthropogenic substances in a rapidly developing tropical island.

Between 1945 and 1998, the population of the city of Papeete increased from 30,000 to more than 120,000 inhabitants (ISTAT, 1996). The extension of Papeete and its harbour (Fig. 1) was completed during the early sixties in conjunction with the development of nuclear testing facilities on the atolls of Mururoa and Fangataufa. The building of harbour facilities was initiated in 1938. However, during the period 1963–1966, a total of almost 100,000 m<sup>2</sup> of land was reclaimed from the sea, coral platforms and barrier reef. The most significant artificial structure is a 2 km long concrete sea wall built on the barrier reef that hampers ocean water inputs over 2/3 of the reef length. As a consequence, water circulation and the rate of lagoon water renewal have been greatly reduced in this part of the lagoon. Moreover, the Papeava and Tipaerui rivers have been delivering increasing loads of terrigenous and anthropogenic material to the lagoon because of increasing soil erosion, industrial effluent discharge and release of mostly untreated waste waters (Fichez et al., 1997). To evaluate the potential significance of these inputs, sediment cores were sampled in 1996 at two different sites corresponding to the eastern and western part of the Papeete harbour area (Fig. 1).

Two cores were sampled by SCUBA diving using a 1 m long and 25 cm diameter PVC corer (Harris, 1998). Core PPV (Fig. 1) was sampled at 34 m depth in the western part of the harbour, which is sheltered by the seawall, and at the mouth of the Papeava River, which collects more than half of the sewage waters released by the city of Papeete. Core PPT (Fig. 1) was sampled at 23 m depth in the eastern and more active part of the harbour (shipping and ship repair), which is also sheltered by the sea wall. Each core was immediately brought back to the laboratory and sliced in 1 cm sediment sections. Depending on analyses, sediment sub-samples were either freeze-dried or oven-dried.

Sediment accumulation rates were determined from the decrease in excess <sup>210</sup>Pb activity. <sup>210</sup>Pb was analysed

\* Corresponding author. Tel.: +33 4 91 04 16 05; fax: +33 4 91 04 16 35.

E-mail address: fichez@com.univ-mrs.fr (R. Fichez).

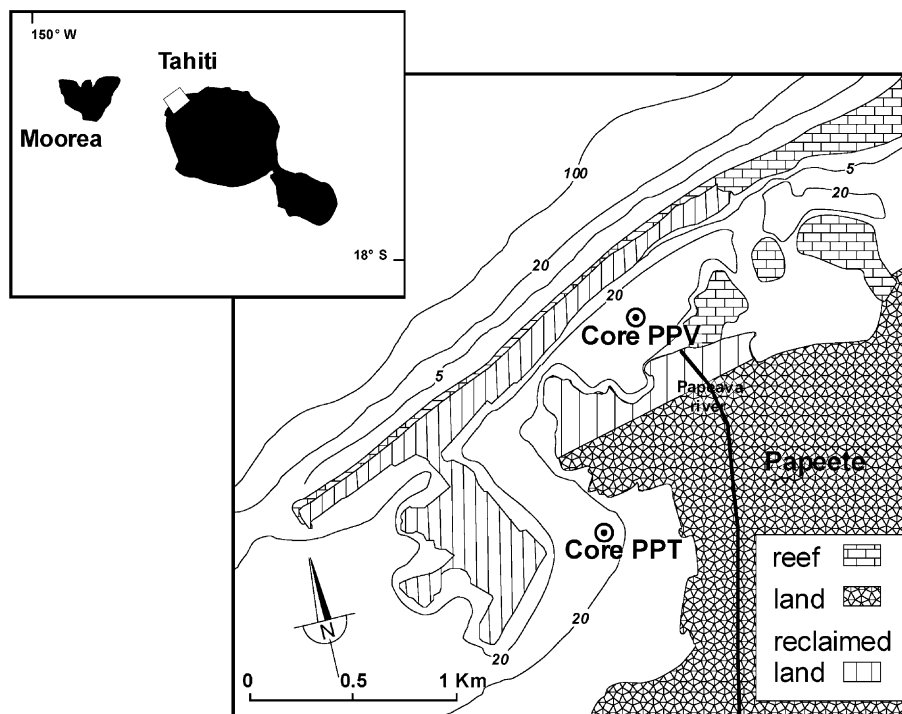


Fig. 1. Map of the lagoon and barrier reef around the city of Papeete with location of core-sampling sites.

in triplicate samples by measuring its granddaughter  $^{210}\text{Po}$ , considered to be in secular equilibrium with  $^{210}\text{Pb}$  (Teksöz et al., 1991). Each sample was spiked with  $^{208}\text{Po}$  in order to appraise possible losses incurred during application of the digestion protocol. The  $^{210}\text{Po}$  measurement was performed in a NUMELEC grid-ded-chamber (NU 114B model) by alpha counting, following the standardised methods of Flynn (1968) modified by Nittrouer et al. (1979) and further adapted to carbonate rich sediments by Serra et al. (1991). Excess  $^{210}\text{Pb}$  was determined as total  $^{210}\text{Pb}$  minus  $^{226}\text{Ra}$  supported  $^{210}\text{Pb}$ . Sediment supported  $^{226}\text{Ra}$  activity was measured using gamma spectrometry. Sediment accumulation rates were determined according to Faure (1986). Mass accumulation of sediment has been commonly used to derive independent depth scale based upon the cumulative weight per unit area ( $\text{g cm}^{-2}$ ) and plotting excess  $^{210}\text{Pb}$  activity versus mass accumulated sediment ( $\text{g cm}^{-2}$ ) rather than simple depth (cm) allows compensation for compaction effects (Bollhöfer et al., 1994). Mass accumulation was determined according to Buesseler and Benitez (1994) after measuring particle density on each sediment sub-sample according to Boyd (1995). The age for each sediment level was derived from the linear regression of excess  $^{210}\text{Pb}$  versus accumulated sediment mass which allowed for the calculation of an average accumulation rate (Robbins and Herche, 1993). However, carbonate, which contains little or no  $^{210}\text{Pb}$ , may be responsible of a significant dilution of the  $^{210}\text{Pb}$  signature. In order to compensate for this bias,

linear regression was conducted on non-carbonate accumulated sediment mass instead of bulk accumulated sediment mass. By doing this we calculated the accumulation rate of terrestrial sediment only, from which a more confident age-depth relationship could be established and subsequently used to calculate bulk sediment accumulation rate and interpret changes in sediment deposition and composition.

An additional coring was conducted on the PPT site to allow for the determination of  $^{137}\text{Cs}$ . Due to low activity levels commonly recorded in the southern hemisphere (Hancock et al., 2002), two additional cores were sampled at station PPT and samples from identical sediment levels were pooled together to allow for the gamma determination of  $^{137}\text{Cs}$ . It must be acknowledged that pooling cores together is a sure way to enhance variability. The distribution of  $^{137}\text{Cs}$  was used to check on the validity of  $^{210}\text{Pb}$ -derived sediment deposition rate taking into account the specific behaviour of  $^{137}\text{Cs}$  in marine sediments of the southern hemisphere (Hancock et al., 2002).

Sediment grain size was analysed using a HR 850-B laser particle sizer over a closed range of 0–600  $\mu\text{m}$ . Sediment samples were washed with water through a 1 mm mesh size sieve and dispersed in water by exposure to ultrasound for 20 s. Results are synthetically presented as the relative distribution in four class sizes: >63  $\mu\text{m}$ , 63–31  $\mu\text{m}$ , 31–3.9  $\mu\text{m}$  and <3.9  $\mu\text{m}$ . Additionally, grain size parameters such as mean size (Mz) and sorting ( $\sigma$ ) were calculated (Wentworth, 1922; Folk and Ward,

1957; Rivière, 1977). The water content expressed in percent of sediment wet weight was obtained by weighing sediment samples before ( $W_w$ ) and after ( $W_d$ ) drying in an oven at 105 °C for 48 h (UNEP/IOC/IAEA, 1995).

Calcium carbonate content was extracted using acetic acid as described by Loring and Rantala (1992) and measuring Ca in the extract. The acetic attack method was selected because it is one of the weakest chemical treatments that can be used to dissolve calcium carbonate (Loring and Rantala, 1988). Ca was analysed on a Varian spectrometer model SpectrAA 400 using the flame technique. This method provided consistent results whereas the measurement of weight loss after acidification strongly overestimated carbonate content due to the joint degradation of organic material and oxides (Harris, 1998).

The determination of organic carbon was used to assess sediment organic content. Sediment carbonate was removed according to the hydrochloric acid vapour technique (Yamamuro and Kayanne, 1995) prior to analysis on a Perkin Elmer 2400 CHN Elemental Analyser.

Metal concentrations were determined in the fine sediment fraction (<63  $\mu\text{m}$ ) obtained by wet sieving. Sediment samples were subject first to an acetic acid extraction step identical to that used to extract carbonates. The proportion of metal removed by this extraction is operationally defined as the non-detrital (acid soluble) metal fraction of the sediment and corresponds to a chemical assessment of the bio-available fraction of sedimentary metals. The remaining fraction, operationally defined as the residual (acid insoluble) fraction (UNEP/IOC/IAEA, 1995), was obtained by further subjecting the sediment sample to fluorhydric acid attack according to Tessier et al. (1979). Concentrations of Cr, Ni, Mn, Fe, Al, Pb, Cu, and Zn in each fraction were determined on a Varian spectrometer model SpectrAA 400 using the flame technique. In addition, certified reference materials (SD-M-2/TM from International Atomic Energy Agency; NRCC-BCSS-1 from National Research Council of Canada) were analysed to check for extraction efficiency. Reproducibility controls were conducted on triplicate samples to assess mean concentration and standard deviation.

To synthesise the complex data set generated, we conducted a principal component analysis (PCA) combined with a cluster analysis yielding a classification of the normalized data as a function of the main sources of influence. The PCA was conducted on a matrix of 20 variables for 33 sediment samples and the cluster analysis was conducted on the correlation matrix resulting from the PCA.

Excess  $^{210}\text{Pb}$  activity was plotted on a log scale versus non-carbonate accumulated sediment mass for each sediment core (Fig. 2) and average sedimentation and sediment accumulation rates were calculated from the linear portions of the plots (Table 1). Both PPV and

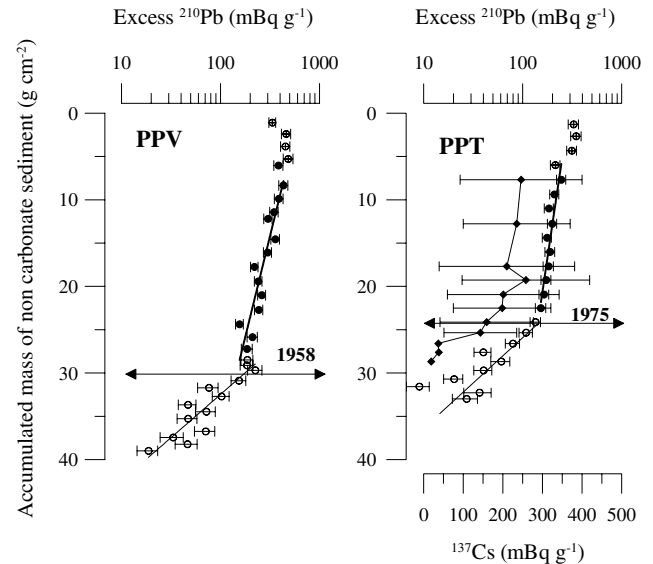


Fig. 2. Radioisotope distribution in cores PPV and PPT. Log of excess  $^{210}\text{Pb}$  activity is plotted on a logarithmic scale versus accumulated sediment mass ( $\text{g cm}^{-2}$ ) (● and ○ represent data used for linear fits, □ represents discarded data) for both cores. Additional  $^{137}\text{Cs}$  activity (◆) has been determined and plotted for core PPT alone to check on the validity of  $^{210}\text{Pb}$ -derived sediment deposition rate.

Table 1

Mean sedimentation rate and sediment accumulation rate in cores PPV and PPT

Localisation	$\text{mm y}^{-1}$	$\text{g cm}^{-2} \text{y}^{-1}$
Core PPV after 1958	$10 \pm 1$	$0.92 \pm 0.09$
Core PPV prior to 1958	$3 \pm 0.5$	$0.38 \pm 0.06$
Core PPT after 1975	$14 \pm 1$	$1.89 \pm 0.18$
Core PPT prior to 1975	$2 \pm 0.5$	$0.30 \pm 0.04$

PPT cores presented a top layer (0–6  $\text{g cm}^{-2}$ ) with homogeneous excess  $^{210}\text{Pb}$  activities. This homogeneous layer is generated by mixing processes with short time scales when compared with the  $^{210}\text{Pb}$  half life of 22.3 years (Koide et al., 1973). Due to the absence of significant wave effects in the protected lagoon, bioturbation can be considered as the sole significant process contributing to such mixing. Below this top section, both cores PPV and PPT presented two very distinct layers corresponding to distinct excess  $^{210}\text{Pb}$  activity profiles, and hence distinct sediment deposition rates.

In core PPV, the first layer extending between 6  $\text{g cm}^{-2}$  and 27  $\text{g cm}^{-2}$  showed a decrease in excess  $^{210}\text{Pb}$  from 386  $\text{mBq g}^{-1}$  to 186  $\text{mBq g}^{-1}$ . Below 27  $\text{g cm}^{-2}$  the activity decreased more rapidly down to 19  $\text{mBq g}^{-1}$  at 39  $\text{g cm}^{-2}$ . The linear regression analysis for each of the two distinctive sections yielded average non-carbonate sediment accumulation rates of  $0.71 \text{ g cm}^{-2} \text{y}^{-1}$  in the upper part and  $0.17 \text{ g cm}^{-2} \text{y}^{-1}$  in the lower part, corresponding to bulk sediment accumulation rates of  $0.92 \text{ g cm}^{-2} \text{y}^{-1}$  and  $0.38 \text{ g cm}^{-2} \text{y}^{-1}$ , respectively. The two linear fits intersected at 29  $\text{g cm}^{-2}$  corresponding to

year 1958 ( $\pm 4$  y) and a bulk sediment depth of 38 cm. The sedimentation rate in the top of the core was estimated at  $1 \text{ cm y}^{-1}$  and the whole core length represented 150 years of sediment deposition.

In core PPT, the first layer extending between  $6 \text{ g cm}^{-2}$  and  $24 \text{ g cm}^{-2}$  showed a decrease in excess  $^{210}\text{Pb}$  from  $245 \text{ mBq g}^{-1}$  to  $153 \text{ mBq g}^{-1}$ . Below  $24 \text{ g cm}^{-2}$  the activity decreased more rapidly down to  $27 \text{ mBq g}^{-1}$  at  $35 \text{ g cm}^{-2}$ . The linear regression analysis for each of the two distinctive sections yielded average non-carbonate sediment accumulation rates of  $1.16 \text{ g cm}^{-2} \text{ y}^{-1}$  in the upper part and  $0.09 \text{ g cm}^{-2} \text{ y}^{-1}$  in the lower part, corresponding to bulk sediment accumulation rates of  $1.89 \text{ g cm}^{-2} \text{ y}^{-1}$  and  $0.30 \text{ g cm}^{-2} \text{ y}^{-1}$ , respectively. The two linear fits intersected at  $23 \text{ g cm}^{-2}$  corresponding to year 1975 ( $\pm 3$  y) and a bulk sediment depth of 29 cm. The sedimentation rate in the top of the core was estimated at  $1.4 \text{ cm y}^{-1}$  and it was calculated that the whole core length represented 120 years of sediment deposition.

Calculation of sedimentation rates based on excess  $^{210}\text{Pb}$  correspond to a maximum estimate as various mixing processes also contribute to the distribution of  $^{210}\text{Pb}$  in the sediment (Robbins and Herche, 1993). Therefore, the distribution of  $^{137}\text{Cs}$  in core PPT was used to test the  $^{210}\text{Pb}$  chronology by comparing the age assignment of the  $^{137}\text{Cs}$  horizon (deepest level where activity can be detected) against a 1952 date of onset of atmospheric nuclear testing (Hancock et al., 2002). The distribution of  $^{137}\text{Cs}$  in core PPT (Fig. 2) showed homogeneous low values around  $200 \text{ mBq g}^{-1}$  above  $40 \text{ g cm}^{-2}$  (30 cm) plus large standard deviation, the latter being partly attributed to core pooling. In the Southern Hemisphere,

core profiles are not expected to show a sharp  $^{137}\text{Cs}$  1963 peak, but rather a broad plateau of low activity in the upper part of cores followed by a sharp decrease to almost undetectable levels corresponding to the pre-atmospheric nuclear testing period dated prior to 1952 (Hancock et al., 2002). Detection limits in  $^{137}\text{Cs}$  activity were reached at  $42 \text{ g cm}^{-2}$  corresponding to a depth of 30 cm and a calculated date of 1956 ( $\pm 5$  y). This pattern in the distribution of  $^{137}\text{Cs}$  confirms and validates  $^{210}\text{Pb}$  chronology in core PPT. Due to convergent patterns between the two cores it was considered that this validation could be reasonably extended to core PPV.

Grain size distribution (Fig. 3) in cores PPV and PPT showed that sediments were essentially composed of material below  $63 \mu\text{m}$ . In core PPV, we observed that, except for the deeper layer, sand contributed to less than 10% and disappeared after 1960 together with an increase in the  $31\text{--}63 \mu\text{m}$  fractions. In core PPT, the contribution of sand to sediment composition sharply decreased from around 25% below 40 cm (hence prior to year 1900) to 2% in the upper and most recent sediment layer. This trend is paralleled by an increase in the percentage of  $3.9\text{--}31$  and  $31\text{--}63 \mu\text{m}$  fractions.

Grain size parameters, water content, calcium carbonate and organic carbon concentrations were plotted as a function of sediment depth (Fig. 4). In core PPV the distribution of mean size ( $Mz$ ) and sorting ( $\sigma i$ ) was heterogeneous showing 3 distinctive layers. From the bottom to 50 cm depth, sediment shifted from medium silt ( $Mz = 5.7\Phi$ ) to very fine silt ( $Mz = 7.6\Phi$ ) and from very poorly sorted ( $\sigma i = 2.5\Phi$ ) to moderately sorted ( $\sigma i = 1.6\Phi$ ). Between 50 and 42 cm depth there was a shift

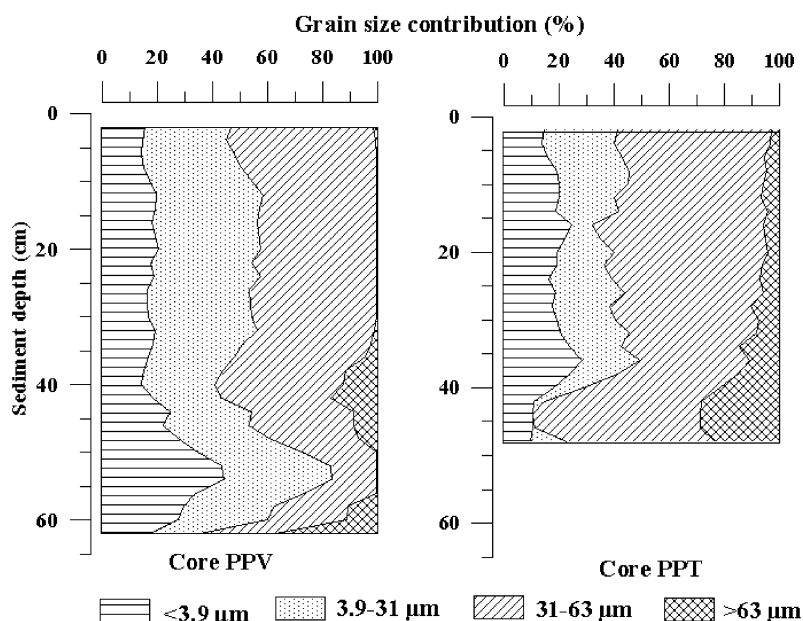


Fig. 3. Grain size distribution expressed in percent of dry weight versus sediment depth in cores PPV and PPT.

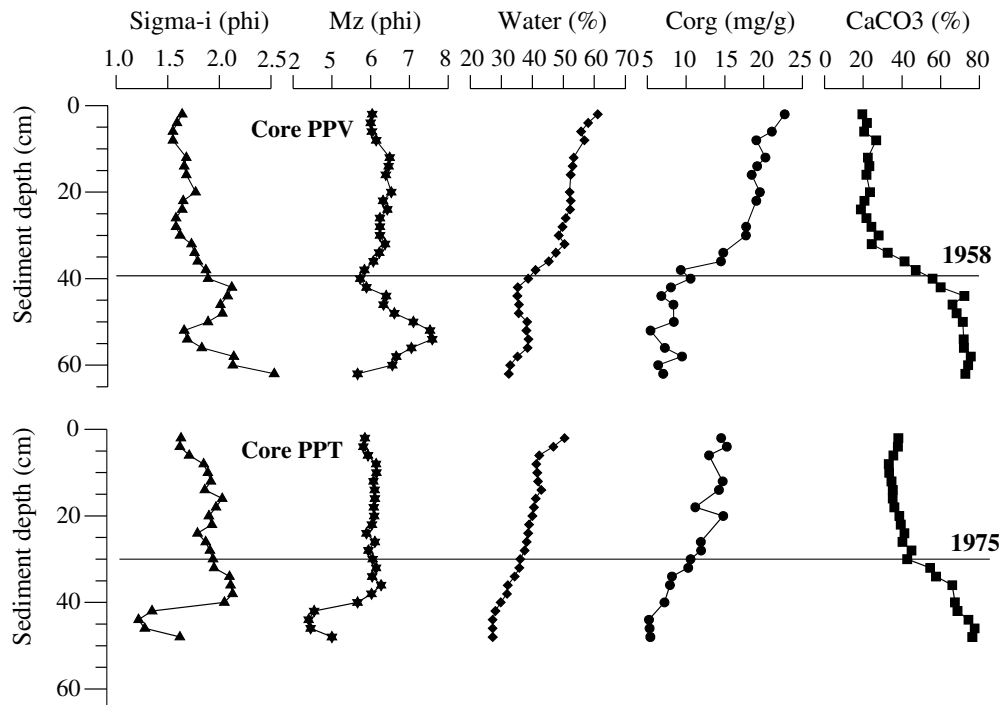


Fig. 4. Mean size (Sigma-i), sorting (Mz), water content (water), organic carbon (C-org), and calcium carbonate ( $\text{CaCO}_3$ ) versus sediment depth in cores PPV, and PPT.

back to medium silt ( $Mz = 5.7\Phi$ ) and to very poorly sorted sediments ( $\sigma_i = 2.1\Phi$ ). Above 40 cm depth, hence since 1958, there was little change in medium size and a slight improvement in sorting. In core PPT we observed a strong shift in Mean size from coarse silt ( $Mz = 4.4\Phi$ ) to fine silt ( $Mz = 6.3\Phi$ ) and from poorly sorted ( $\sigma_i = 1.2\Phi$ ) to very poorly sorted ( $\sigma_i = 2.0\Phi$ ) between the bottom of the core and 40 cm depth with little change afterward.

Water content in cores PPV and PPT increased from 28–35% in the deeper to 50–60% in the upper layers. This change in sediment water content is a logical consequence of compaction due to sediment accumulation.

According to a classification established in the Great Barrier Reef and based on sediment calcium carbonate contribution (Maxwell, 1968), sediment in cores PPV and PPT shifted from impure carbonate sediment (>70% carbonate) in the older levels to transitional/terrigenous sediments ( $\approx 40\%$  carbonate) and terrigenous sediments (<22% carbonate) in the modern levels of cores PPT and PPV, respectively.

The distribution of organic carbon increased from past to present with a difference of  $17 \text{ mg g}^{-1}$  in core PPV and  $12 \text{ mg g}^{-1}$  in core PPT. This difference is related to the combination of diagenetic alteration and changes in organic material inputs (Harris et al., 2001).

Evolution of metal concentrations was studied in cores PPV and PPT as they provided reliable geochronological records. The down-core distribution of Cr,

Ni, Mn, Fe, Al, Pb, Cu, Zn in the exchangeable and refractory phases is presented in Fig. 5.

In cores PPV and PPT, all metals from the residual phase increased from the bottom to the top of the cores, hence from past to present. The exchangeable phase presented more diverse distribution patterns. In core PPV, Cr decreased from past to present, Ni and Al were almost constant around  $22 \mu\text{g g}^{-1}$  and  $1 \text{ mg g}^{-1}$ , respectively, while all other metals (Mn, Fe, Pb, Cu, Zn) increased. In the exchangeable phase of core PPT, Cr decreased slightly from past to present, Ni was almost constant around  $24 \mu\text{g g}^{-1}$  while all other metals (Mn, Fe, Al, Pb, Cu, Zn) increased. From past to present, the contribution of the exchangeable phase relative to bulk metal concentrations in core PPV decreased from 26% to 4% for Cr, 35% to 10% for Ni, 33% to 23% for Mn and 5% to 1.8% for Al. It was almost constant at 3% for Fe and it increased from 7% to 12% for Pb, 8% to 18% for Cu and 13% to 36% for Zn. In core PPT, the contribution of the exchangeable phase decreased from past to present, from 10% to 4% for Cr, 33% to 15% for Ni, and 3% to 1.6% for Al. It was almost constant at 3% for Fe, 17% to 23% for Mn, 14% to 17% for Pb, 10% to 15% for Cu and 25% for Zn.

Considering the convergence between the decrease in exchangeable Cr and the decrease in  $\text{CaCO}_3$ , the  $\text{Cr}_{\text{exch}}/\text{Ca}$  ratio was studied to identify a possible relationship. The average  $\text{Cr}_{\text{exch}}/\text{Ca}$  ratio, calculated on the whole

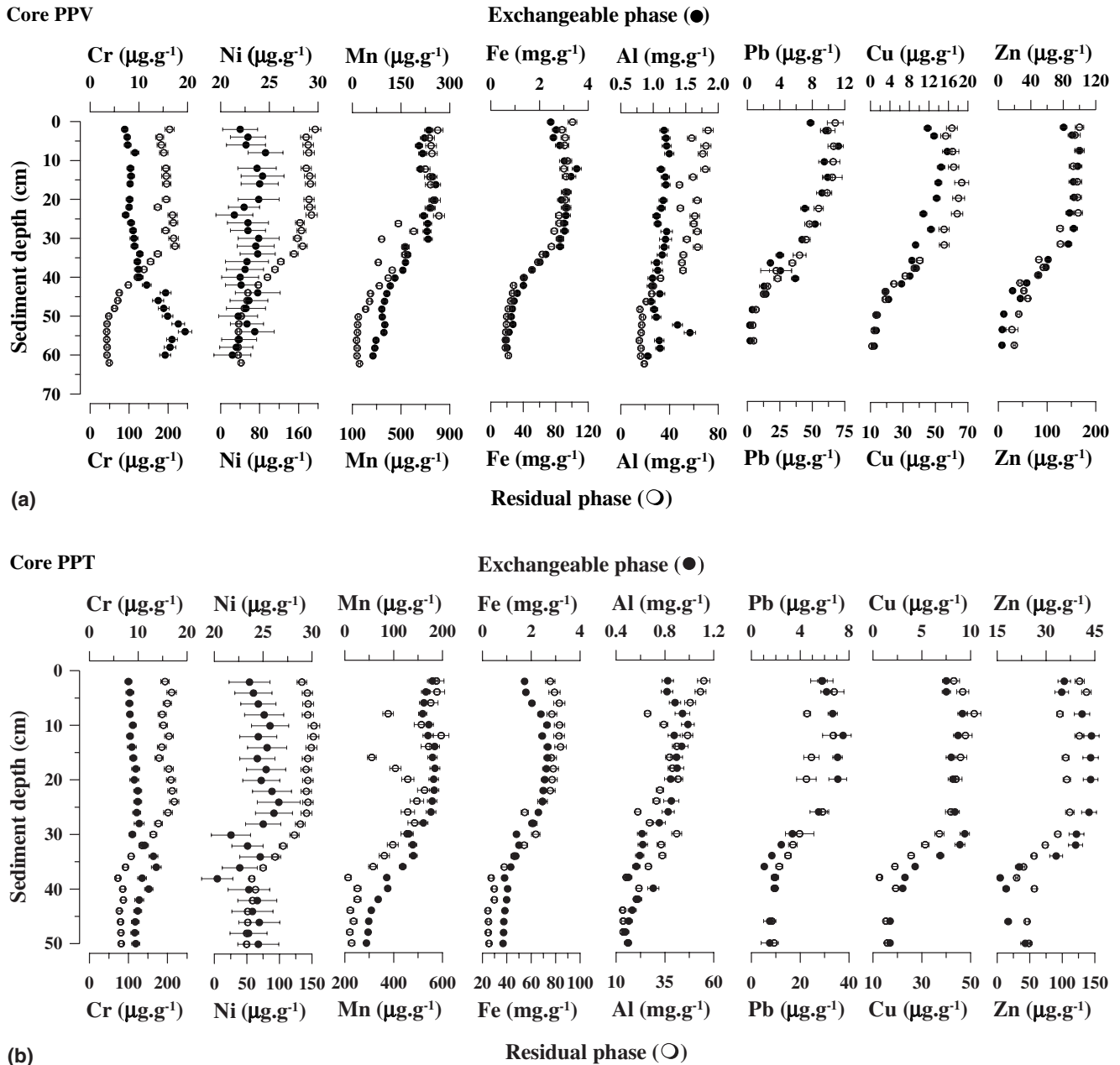


Fig. 5. Evolution of Cr, Ni, Mn, Fe, Al, Pb, Cu and Zn in the exchangeable (● and top x-axis scale) and residual (○ and bottom x-axis scale) phases versus sediment depth in cores PPV (a), and PPT (b).

sediment core, was  $0.07 \pm 0.02$  in core PPV and  $0.05 \pm 0.01$  in core PPT and the very low standard deviation strongly supported the hypothesis of a linkage between exchangeable Cr and  $\text{CaCO}_3$ .

The results from a principal component analysis (PCA) combined with a cluster analysis (Fig. 6) provided a synthetic classification of the samples as a function of the main sources of influence. Axis 1 was mainly related to the sediment  $\text{CaCO}_3$  content and sorting ( $\sigma_i$ ) on the positive side and to organic carbon (C-org) and most metals in either exchangeable or residual phases on the negative side. High carbonate content and sorting on the

positive side can be related to authigenic carbonate production, while high concentrations in metals on the negative side can be related to terrigenous inputs. No specific anthropogenic influence could be detected as no clear differences between combined metal species and geochemical phase could be identified. The authigenic versus terrigenous gradient accounted for 70% of the sample variability. Axis 2, accounting for 12% of the variability, was mainly related to Mn-e and Ni-e on the negative side and Al-e and sediment mean size (Mz) on the positive side. Axis 3 only accounted for 7% of the variability and was mainly related to Mn-e, Mz and sigma-i.

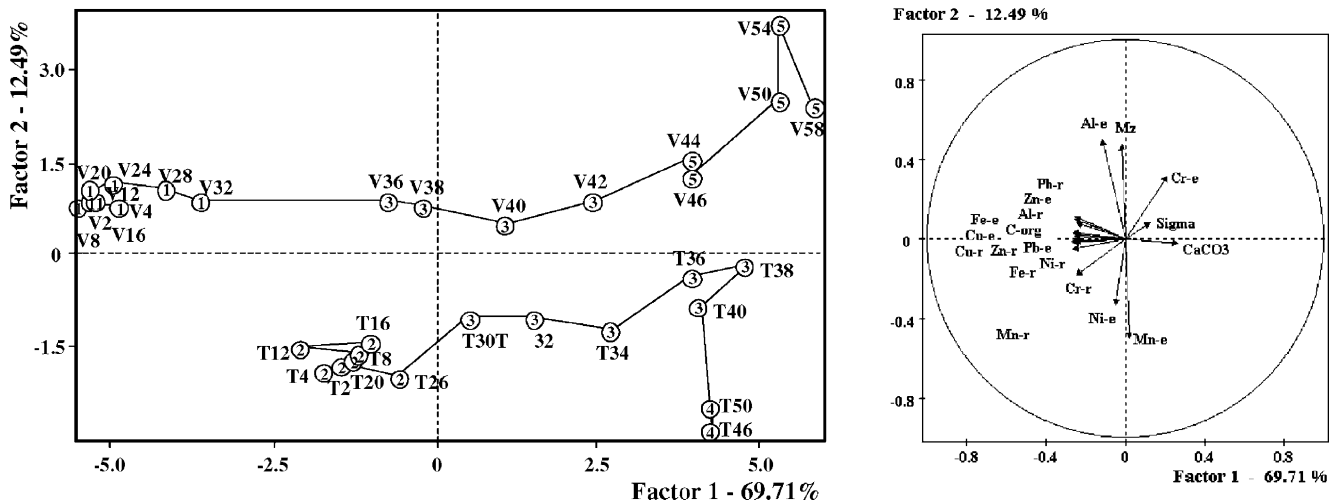


Fig. 6. Combined principal component analysis and cluster analysis based on the sediment characteristics and total metal concentrations in cores PPV and PPT. The figure on the left is a plot of core samples data as a function of axes 1 and 2 (both accounting for 82.2% variability). For each data point the cluster analysis category (circled number) and the core level (V stands for PPV and T for PPT and the associated number indicates sediment depth in cm; i.e. V36 means core PPV level 36 cm) are indicated. The right figure shows a projection of parameters as a function of axis 1 and 2.

Results from the PCA showed that sediment samples from core PPV and PPT were respectively organised along axis 1. There was a clear parallel shift from authigenic to terrigenous origin from the bottom to the top of the core, and hence from past to present. Cluster analysis further allowed for the distinction between five classes. Class 5, with a strong authigenic signature, gathered the five lower sediment layers of core PPV (prior to 1924). Class 4 only gathered two sediment samples from the bottom of core PPT (prior to 1866) which mainly identified from class 3 due to their axis 2 co-ordinates. Class 3 combined samples from core PPV and PPT and displayed a significant and progressive shift from authigenic to slightly terrigenous origins. Class 2 gathered seven sediment samples from core PPT corresponding to the period 1964–1996 that were typified by a moderate terrigenous signature. Class 1 with nine sediment samples from core PPV and from the period 1973–1996 showed the strongest terrigenous influence. Both class 1 and 2 showed reasonably aggregated data demonstrating a progressive stabilisation in the amount and sources of input during the past 30 years.

Carbonate profiles in cores PPT and PPV indicated a strong modification in sediment sources during the period of deposition considered. Sedimentation in a coral reef ecosystem adjacent to a volcanic island like Tahiti depends on two main sources of sediment input. The first is a terrestrial source, mainly in the form of basaltic material rich in silicates, aluminium, iron and manganese, that represents an allochthonous origin. The second is a marine, or more precisely a lagoon authigenic source, identified by carbonate minerals which are formed by calcifying organisms such as corals, calcareous algae, molluscs, etc. that represent an autochthonous origin. It must be acknowledged that carbonates

may not only originate from coral reefs but also, and in a significant proportion, from authigenic lagoon carbonate producers such as foraminifers, molluscs, etc. (Chevillon, 1996).

For the period prior to 1958 in core PPV and 1975 in core PPT (and hence prior to the extensive and recent development of the city and harbour of Papeete,) low sedimentation rates with a high carbonate contribution and low metal concentrations demonstrated that the main source of accumulated sediments was of lagoon authigenic origin. After 1958 in core PPV (level 38 cm) and 1975 in core PPT (level 29 cm), sedimentation in the lagoon was dominated by terrestrial inputs. This predominance was stronger in core PPV, with less than 25% of carbonates, than in core PPT that contained less than 40% carbonates. Metal concentrations showed that terrestrial inputs increased dramatically in the middle of the century with average enrichment factors of around 6 in core PPV and 8 in core PPT (Table 2).

The transition zone between the two very distinct layers extended from 1930 to 1958 in core PPV and from 1946 to 1975 in core PPT. This large transition zone, which goes back to a date that is older than the transformation of Papeete, must be attributed to sediment mixing related to bioturbation (Officer and Lynch, 1989; Kramer et al., 1991). If a modification occurs in the deposition regime of a tracer, biological mixing will favour the burial of the new signatures below the effective layer of deposition. Therefore, the transition zone must be considered as a layer reflecting the combined effects of bioturbation, sediment burial and progressive shift in the amount and nature of deposited sediment.

The results presented in this paper and their synthesis through the joint PCA-cluster analysis strongly suggest that core PPV is located close to a major source of ter-

Table 2

Mean and standard deviation (SD) of fluxes of total metal and Ca in the sediment for cores PPV and PPT prior and after anthropogenic modification of sediment deposition

		Cr	Ni	Mn	Fe	Al	Pb	Cd	Cu	Zn	Ca
PPV 1958–1996	Mean	182	176	781	81,366	55,682	58.4	0.3	63.0	209	107
	SD	19	21	170	10,523	7099	13.0	0.2	10.4	39	32
PPV prior to 1958	Mean	29	27	112	10,119	8028	5.7	0.1	8.4	26	113
	SD	9	7	39	3971	2046	3.8	0.2	3.8	13	11
Enrichment factor		<b>6.3</b>	<b>6.4</b>	<b>7.0</b>	<b>8.0</b>	<b>6.9</b>	<b>10.3</b>	<b>2.3</b>	<b>7.5</b>	<b>7.9</b>	<b>0.9</b>
PPT 1975–1996	Mean	391	318	1258	147,235	73,565	65.2	0.8	102.2	296	283
	SD	24	11	155	16,153	19,368	8.8	1.2	6.8	23	86
PPT prior to 1975	Mean	32	28	112	10,912	6939	4.3	0.1	8.1	25	81
	SD	8	8	35	4140	2915	1.4	0.0	3.5	9	14
Enrichment factor		<b>12.1</b>	<b>11.3</b>	<b>11.2</b>	<b>13.5</b>	<b>10.6</b>	<b>15.0</b>	<b>13.6</b>	<b>12.6</b>	<b>12.1</b>	<b>3.5</b>

Fluxes in  $\mu\text{g cm}^{-2} \text{y}^{-1}$  were obtained by multiplying element concentration by sediment deposition rate (calculated in Table 1). Enrichment factors between the top and bottom layers are presented in bold.

rigeneous and anthropogenic inputs which can be identified as the mouth of the Papeava river. Inputs from this source are primarily discharged in the western part of the harbour but are also partly exported toward the eastern harbour basin where core PPT was sampled. Even though both sites present a parallel increase in terrigenous inputs, no strong geochemical convergence was observed between the two cores, suggesting differences in the sources of inputs. By combining historical data from the study zone and the results from the present study, it is possible to identify the major environmental causes responsible for such changes in sediment deposition.

*Decrease in lagoon water circulation*—The building of Papeete Harbour, funded in 1963, resulted in significant modifications including land reclamation on patch reef, building of embankments and, more importantly, building of a 3 km long jetty on the top of the barrier reef designed to protect the harbour from the large Pacific swell. As a major consequence, water circulation in the Papeete lagoon was significantly altered, the blockade of oceanic inputs over the reef strongly limiting water exchanges and favouring the deposition of fine sediments within the lagoon. Additionally, the reclaimed land strongly reduced water exchange between the western and eastern basins, which now reflect some slight differences in terrigenous input sources.

*Artificial increase in terrigenous inputs*—Urban extension since the end of the fifties generated a global modification of the coastal zone around Papeete (Gabrié, 1995; ORSTOM, 1993). The building of an embankment on the fringing reef, plus the associated channelisation of the Papeava River through the city, strongly modified the discharge system of the river. The extension of the city of Papeete generated the need for housing areas resulting in deforestation and subsequent erosion from the steep slopes of the island. Destruction of the soil layer and associated erosion generated a significant increase in the downstream transport of terrigenous particles towards the lagoon. This mech-

anism is strongly enhanced during the rainy season, when turbidity plumes form at the mouth of rivers. During such periods, particle vertical flow rates may exceed  $1000 \text{ g m}^{-2} \text{ d}^{-1}$ ; a maximum rate of  $3000 \text{ g m}^{-2} \text{ d}^{-1}$  was recorded in September 1995 in front of the mouth of the Papeava river during a major rainfall event (Harris et al., 2001). In naturally open barrier reef lagoons, a large part of this particulate material is rapidly exported toward the ocean through the main reef passes but retention of terrigenous inputs in the lagoon of Papeete is enhanced by artificial lowering in water exchange (see above).

*Anthropogenic inputs of contaminants*—Urban development is coincidental with the release of artificial substances of which metals are a significant component. The Papeava River has been increasingly used as a collector for untreated sewage release and was identified as a major source of phosphorus inputs to the lagoon (Harris et al., 2001). Metals are major by-products of urban development and their adsorption on fine particles will essentially result in a qualitative change in the geochemical composition of deposited sediments.

The results obtained from the sediment archives in Papeete harbour may be considered as an example of how barrier reef lagoons might be locally affected by urban development

## Acknowledgments

Some very special thanks must be addressed to all colleagues from IRD Antropic and Ecotrope programmes. We are also deeply indebted to Marc Treszinski from IPSN-LESE who was extremely supportive regarding radioisotope determination techniques and metal analysis and to Gary Hancock for his revision of the manuscript. This work was funded by IRD and the Ministry of Environment in French Polynesia.

## References

- Aubanel, A., Payri, C., Tatarata, M., 1998. La Polynésie Française. In: L'état des récifs coralliens en France Outre-Mer, Secrétariat d'Etat à l'Outre-Mer, Paris, pp. 59–73.
- Bollhöfer, A., Mangiri, A., Lenhard, A., Wessels, M., Giovanoli, F., Schwarz, B., 1994. High-resolution  $^{210}\text{Pb}$  dating of Lake Constance sediments: stable lead in Lake Constance. *Environ. Geol.* 24, 267–274.
- Boyd, C.E., 1995. Bottom Soils, Sediment, and Pond Aquaculture. Chapman & Hall, New York, p. 322.
- Buesseler, K.O., Benitez, C.R., 1994. Determination of mass accumulation rates and sediment radionuclide inventories in the deep Black Sea. *Deep-Sea Res.* I 41, 1605–1615.
- Chenhall, B.E., Yassini, I., Depers, A.M., Caitcheon, G., Jones, B.G., Batley, G.E., Ohmsen, G.S., 1995. Anthropogenic marker evidence for accelerated sedimentation in Lake Illawarra, New South Wales, Australia. *Environ. Geol.* 26, 124–135.
- Chevillon, C., 1996. Skeletal composition of lagoonal modern sediments in New Caledonia: Coral, a minor constituent. *Coral Reefs* 15, 199–207.
- Cornwell, J.C., Conley, D.J., Owens, M., Stevenson, J.C., 1996. A sediment chronology of the eutrophication of Chesapeake Bay. *Estuaries* 19, 488–499.
- Faure, G., 1986. Principles of Isotope Geology. John Wiley & Sons, Inc., New York.
- Fichez, R., Harris, P., Jouen, R., Badie, C., Fernandez, J.M., 1997. Sedimentary records of human induced environmental changes in the Tahiti lagoon. In: Proceedings of the 8th International Coral Reef Symposium, Panama 2, pp. 1833–1838.
- Flynn, W.W., 1968. Determination of low levels of polonium-210 in environmental materials. *Anal. Chem.* Acta 43, 221–227.
- Folk, R.L., Ward, W.C., 1957. Brazos river bar: a study of significance of grain size parameters. *J. Sedim. Petrol.* 27, 3–26.
- Gabrié, C., 1995. L'état de l'environnement dans les territoires français du pacifique sud. Rapport du Ministère de l'Environnement, Paris, 121 p.
- Gerritse, R., Hernandez, F., Murray, A.S., Wallbrink, P.J., Brunskill, G., 1995. Distribution of organochlorines, polycyclic aromatic hydrocarbons, phosphorus and  $^{137}\text{Cs}$  in sediment profiles from Ellen Brook in Western Australia. *Mar. Fresh. Res.* 46, 843–851.
- Grousset, F.E., Jouanneau, J.M., Castaing, P., Lavaux, G., Latouche, C., 1999. A 70 year Record of contamination from industrial activity along the Garonne River and its tributaries (SW France). *Estuar. Coast. Shelf Sci.* 48, 401–414.
- Hancock, G., Edgington, D.N., Robbins, J.A., Smith, J.N., Brunskill, G., Pfitzner, J., 2002. Workshop on radiological techniques in sedimentation studies: methods and applications. In: Fernandez, J.M., Fichez, R. (Eds.), Environmental Changes and radioactive tracers, IRD Editions, Paris, France, pp. 233–251.
- Harris, P., 1998. Modification des caractéristiques chimiques du lagon de Papeete liées à l'activité humaine: intérêt des traceurs sédimentaires géochimiques et biogéochimiques dans la reconstitution de l'évolution de l'environnement au cours du XX<sup>e</sup> siècle. These de Doctorat de l'Université Française du Pacifique, 292 p.
- Harris, P., Fichez, R., Fernandez, J.M., Golterman, H.L., Badie, C., 2001. Using geochronology to reconstruct the evolution of particulate phosphorus inputs during the past century in the Papeete Lagoon (French Polynesia). *Oceanol. Acta* 24, 1–10.
- Hutchings, P.A., Payri, C., Gabrié, C., 1994. The current status of coral reef management in French Polynesia. *Mar. Poll. Bull.* 29, 26–33.
- ISTAT 1996. Recensement général de la population de 1996 en Polynésie Française. Premiers résultats. Papeete, 4 p.
- Koide, M., Bruland, K.W., Goldberg, E.D., 1973. Th-228/Th-232 and Pb-210 geochronologies in marine and lake sediments. *Geochim. Cosmochim. Acta* 37, 1171–1187.
- Kramer, K.J.M., Misdorp, R., Berger, G., Duijts, R., 1991. Maximum pollutant concentrations at the wrong depth: a misleading pollution history in a sediment core. *Mar. Chem.* 36, 183–198.
- Loring, D.H., Rantala, R.T.T., 1988. An intercalibration exercise for trace metals in marine sediments. *Mar. Chem.* 24, 13–28.
- Loring, D.H., Rantala, R.T.T., 1992. Manual for the geochemical analyses of marine sediments and suspended particulate matter. *Earth-Sci. Rev.* 32, 235–283.
- Maxwell, W.G.H., 1968. Atlas of the Great Barrier Reef. Elsevier, Amsterdam, 258 p.
- Nittrouer, C.A., Sternberg, R.W., Carpenter, R., Bennett, J.T., 1979. The use of  $^{210}\text{Pb}$  geochronology as a sedimentological tool: application to the Washington continental shelf. *Mar. Geol.* 31, 297–316.
- Officer, C.B., Lynch, D.R., 1989. Bioturbation, sedimentation and sediment–water exchanges. *Estuar. Coast. Shelf Sci.* 28, 1–12.
- ORSTOM 1993. Atlas de la Polynésie Française. Editions IRD, Bondy, France, 112 p.
- Rivière, A., 1977. Méthodes granulométriques techniques et interprétations. Masson, Paris, 170 p.
- Robbins, J.A., Herche, L.R., 1993. Models and uncertainty in Pb-210 dating of sediments. *Verh. Int. Verein. Limnol.* 25, 217–222.
- Serra, C., Poletiko, C., Badie, C., 1991. Contribution à l'étude de la vitesse de dépôt des sédiments en certains plans d'eau de Polynésie Française. Rapport CEA-R-5558, Editions du CEA, Tahiti, 37 p.
- Teksöz, G., Yetis, U., Tuncel, G., Balkas, T.I., 1991. Pollution chronology of the golden horn sediments. *Mar. Poll. Bull.* 22, 447–451.
- Tessier, A., Campbell, P.G.C., Bisson, M., 1979. Sequential extraction procedure for the speciation of particulate trace metals. *Anal. Chem.* 51, 844–851.
- UNEP 1995. Manual for the geochemical analyses of marine sediments and suspended particulate matter. Reference methods for marine pollution studies 63, 74 p.
- Valette-Silver, N.J., 1993. The use of sediment cores to reconstruct historical trends in contamination of estuarine and coastal sediments. *Estuaries* 16, 577–588.
- Wakeham, S.G., 1996. Aliphatic and polycyclic aromatic hydrocarbons in Black Sea sediments. *Mar. Chem.* 53, 187–205.
- Wentworth, C.K., 1922. A scale of grade and class terms for clastic sediments. *J. Geol.* 30, 377–392.
- Yamamuro, M., Kayanne, H., 1995. Rapid direct determination of organic carbon and nitrogen in carbonate-bearing sediments with a Yanaco MT-5 CHN analyser. *Limnol. Oceanogr.* 40, 1001–1005.
- Zwolsman, J.J.G., Berger, G.W., Van Eck, G.T.M., 1993. Sediment accumulation rates, historical input, postdepositional mobility and retention of major elements and trace metals in salt marsh sediments of the Scheldt estuary, SW Netherlands. *Mar. Chem.* 44, 73–94.